Eur. J. Mineral., 37, 63–74, 2025
https://doi.org/10.5194/ejm-37-63-2025

European Journal of Mineralogy
Open Access

Andreybulakhite, $Ni(C_2O_4) \cdot 2H_2O$, the first natural nickel oxalate

Oleg S. Vereshchagin[1], Sergey N. Britvin[1,2], Dmitrii V. Pankin[1], Marina S. Zelenskaya[1], Maria G. Krzhizhanovskaya[1], Maria A. Kuz'mina[1], Natalia S. Vlasenko[1], and Olga V. Frank-Kamenetskaya[1]

[1]Saint Petersburg State University, Universitetskaya Emb. 7/9, Saint Petersburg, 199034, Russia
[2]Kola Science Center, Russian Academy of Sciences, Fersman Str. 14, Apatity, 184200, Russia

Correspondence: Oleg S. Vereshchagin (o.vereshchagin@spbu.ru)

Received: 9 October 2024 – Revised: 11 December 2024 – Accepted: 15 December 2024 – Published: 11 February 2025

Abstract. Andreybulakhite, ideally $Ni(C_2O_4) \cdot 2H_2O$, is a new member of the humboldtine group, named in honour of Andrey Glebovich Bulakh of Saint Petersburg State University. The mineral was discovered at the Nyud-II (Nud-II) Cu–Ni sulfide deposit, Monchegorsk mafic–ultramafic pluton, Kola Peninsula, Russia. Andreybulakhite forms segregations of platy to prismatic crystals up to $2 \times 1 \times 1$ µm in size that are localized in the upper part of the fruiting bodies (apothecia) of *Lecanora* cf. *polytropa* lichen, whose colonies overgrow the oxidized surfaces of pyrrhotite–pentlandite–chalcopyrite ore. The mineral is monoclinic, with space group $C2/c$, $a = 11.8392(5)$ Å, $b = 5.3312(2)$ Å, $c = 9.8357(7)$ Å, $\beta = 126.723(5)°$, $V = 497.59(3)$ Å^3 and $Z = 4$. The Raman spectrum of andreybulakhite contains the following bands (cm^{-1}): 1701 (C=O stretching vibrations and/or multiphonon processes); 1621 (H_2O bending vibrations); 1454 and 924 (C–O and C–C stretching modes); 597 (Ni–O stretching, C–C–O and O–C–O bending vibrations); and 550, 307 and 226 (predominantly Ni–O stretching and deformation modes). The absorption bands of the infrared spectrum are (cm^{-1}) 3389 (O–H stretching vibrations), 1640 (H_2O bending vibrations), 1357 and 1315 (C–O stretching, C–C stretching), and 818 (Ni–O stretching, C–O and C–C stretching, C–C–O and O–C–O bending vibrations). The empirical formula calculated on the basis of $(Ni + Cu + Mg + Co) = 1$ atom per formula unit is $(Ni_{0.63}Cu_{0.27}Mg_{0.08}Co_{0.02})_{\Sigma 1.00}(C_2O_4) \cdot 2H_2O$. The absence of iron in the mineral is a result of oxidative Ni^{2+}/Fe^{3+} fractionation during the secondary aqueous alteration of Ni- and Cu-rich sulfides. Andreybulakhite has synthetic Ni and Co counterparts; the latter implies the possibility of formation of its Co analogue in a related cobalt-rich environment.

1 Introduction

Oxalates are probably the most widespread organic minerals (e.g. Krivovichev, 2021), whose first discoveries in nature were in the 19th century (Breithaupt, 1820). The most common by far are Ca-oxalates: weddellite, $Ca(C_2O_4) \cdot (2.5 - x)H_2O$, and whewellite, $Ca(C_2O_4) \cdot H_2O$ (Ralph et al., 2024). However, more than a half of known natural oxalates contain transition metal (Me) cations (Me denotes Fe, Mn, Cu, etc.) as the species-defining constituents (Ralph et al., 2024). These Me-rich oxalates were primarily discovered in pegmatites (e.g. humboldtine, $Fe^{2+}(C_2O_4) \cdot 2H_2O$; Breithaupt, 1820) but were shown to widely occur as biominerals in various environments (e.g. Clarke and Williams, 1986; Frank-Kamenetskaya et al., 2019; Giester et al., 2023).

Oxalic-acid-producing organisms (mainly fungi) can tolerate different pollutants (including heavy metals; e.g. Fomina et al., 2005; Gadd et al., 2014; Vlasov et al., 2020; Burford et al., 2003), which make them perfect bioweathering agents in various Me-rich deposits. During their lifespans, fungi are capable of dissolving the Me-bearing primary substrate minerals and accumulate the eluted cations in the form of water-insoluble and biologically safe Me-rich oxalates (e.g. Clarke and Williams, 1986; Frank-Kamenetskaya et al., 2019; Vereshchagin et al., 2023). In vitro experiments have shown that fungi can be used in bioremediation of Pb-, Co-

and Ni-rich soils (Huang et al., 2023; Jarosz-Wilkolazka and Gadd, 2003; Magyarosy et al., 2002). However, fungi themselves rarely colonize rocks in amounts sufficient to produce large quantities of oxalic acid. In contrast, lichens, which are symbiotic organisms consisting of algae and fungi, can form large biological mats (van Zuijlen et al., 2020). Detailed studies of lichen have shown that metal oxalates are their typical companions (e.g. Frank-Kamenetskaya et al., 2021; Purvis, 2014, 1984), and lichen can colonize rocks of various compositions (Adamo and Violante, 2000; Estroff, 2008; Frank-Kamenetskaya et al., 2019).

During fieldwork with students on the Nyud-II deposit, Monchegorsk mafic–ultramafic pluton (Monchepluton), Kola Peninsula, Russia (67°53′14″ N, 32°54′4″ E), in 2020, we discovered samples of Cu–Ni ore colonized by *Lecanora* cf. *polytropa* lichens. Further research showed that the fruiting bodies of these lichens (apothecia) contain aqueous nickel oxalate, which was named andreybulakhite (Cyrillic: андрейбулахит) in honour of Andrey Glebovich Bulakh (Cyrillic: Андрей Глебович Булах) (1933–2020), Head of the Department of Mineralogy of Saint Petersburg State University (1987–1992); Head of the New Minerals Commission of the Russian Mineralogical Society; the representative of Russia in the Commission on New Minerals, Nomenclature and Classification (CNMNC) of the International Mineralogical Association (IMA) (1994–2009); honorary member of the Russian (1999) and the Ukrainian (2011) mineralogical societies; and an honorary professor of Saint Petersburg State University (2011). His research interests included (but were not limited to) the mineralogy of the carbonatites of the Kola Peninsula, the alkaline massifs of Yakutia, and issues of natural stone in architecture (Bulakh et al., 2020, 1998; Bulakh and Ivanikov, 1996). He is also the author of a series of textbooks on mineralogy (Wenk and Bulakh, 2016). The mineral and name have been approved by the CNMNC of the IMA under number 2023-037. The holotype specimen is deposited at the Mineralogical Museum of the Department of Mineralogy, Saint Petersburg State University, Saint Petersburg, Russia, catalogue number ML OF-978.

2 Occurrence

Monchepluton is among the most famous geological objects of the Kola Peninsula, where about 100 years ago a series of promising Cu–Ni deposits were found (Fersman, 1941) and a number of minerals were discovered (Genkin et al., 1963; Grokhovskaya et al., 2019; Vymazalová et al., 2020). Today ∼ 10 economic deposits/manifestations of platinum group element (PGE)–Cu–Ni–Cr ores have been described in Monchepluton (Karykowski et al., 2018; Chashchin et al., 2023, 2021; Chashchin and Ivanchenko, 2022). Monchepluton covers an area of ∼ 50 km^2 and is located in the southern part of the Kola Peninsula. The intrusion is Paleoproterozoic (∼ 2.50 Ga), is confined to the Imandra–Varzuga greenstone belt and lies on the Archean basement (Chashchin et al., 2023, 2021; Gorbunov et al., 1981). The rocks of the Monchepluton intrusions are usually unmetamorphosed but magmatically layered. The eastern part of the pluton consists of eastern–western branching (∼ 11 × 3 km) and includes Vuruchuaivench, Poaz, Sopcha and Nyud intrusions. The Nyud intrusion consists of melanocratic norite (bottom part; up to 300 m thick), an olivine horizon (middle part; 6 km long and 100 m thick) and mesocratic norite (upper part; up to 350 m thick; Chashchin et al., 2023). The olivine horizon has ubiquitous fine-sulfide dissemination and includes orthopyroxenite, plagio-orthopyroxenite and melanonorite with varying olivine content (up to 30 vol %; Chashchin et al., 2023).

The Nyud-II deposit was discovered in 1931 by M. Shestopalov and I. Kholmyansky and was developed by open-pit mining in the period of 1969–1974 (Chashchin et al., 2021; Fersman, 1941; Gorbunov et al., 1981). The ore body is a so-called "critical" horizon, which lies above the olivine horizon, in the western part of the Nyud intrusion. It received its name by analogy with the critical zone of the Bushveld complex and in connection with its complex structure, caused by the alternation of rocks of different composition and granularity, in contrast to the monotonous melanocratic norites of the lower zone and normal norites of the upper zone of the Nyud intrusion (Chashchin et al., 2021). Disseminated ores, vein-disseminated ores and schlieren ores predominate. The main ore minerals are pentlandite, $(Ni,Fe)_9S_8$; chalcopyrite, $CuFeS_2$; pyrrhotite, $Fe_{1-x}S$; and magnetite, $FeFe_2O_4$. The veins of continuous sulfides have a length of up to 30 m and a maximum thickness of up to 40 cm. In solid (schlieren) ores, the nickel content is maximum and prevails over copper. The total ore reserves amounted to about 1×10^6 t: 3750 t for Ni and 3000 t for Cu with an average content of 0.37 wt % for Ni and 0.30 wt % for Cu (Chashchin et al., 2021). The deposit is opened by a small quarry in which outcrops of solid (schlieren) sulfide ores (pyrrhotite/pentlandite) are still preserved on the daylight surface.

It was suggested that the sulfide ore formation occurred as a result of the separation of immiscible sulfide liquid during the cooling of sulfur-saturated basic silicate magma (Chashchin et al., 2021). Subsequent fractional crystallization of the sulfide liquid contributed to the non-uniform distribution of Ni, Cu and PGEs. Native osmium and erlichmanite, OsS_2, were released at the early stage (1100–1000 °C), while crystallization of Pt–Fe alloys; sperrylite, $PtAs_2$; and various sulfoarsenides (e.g. irarsite, (Ir,Ru,Rh,Pt)AsS, and hollingworthite, (Rh,Pt,Pd)AsS) and separation of residual sulfide melt occurred at significantly lower temperatures (∼ 600 °C). The ore formation process ended with complete crystallization of the Cu–Ni–Fe sulfides (e.g. pentlandite and chalcopyrite) and the formation of bismuth tellurides (e.g. moncheite, $Pt(Te,Bi)_2$, and kotulskite, $Pd(Te,Bi)_{2-x}$) at lower temperatures (600–400 °C; Chashchin et al., 2021). Andreybulakhite was found in *Lecanora* cf. *polytropa* lichen,

Table 1. Chemical data (in wt %) for andreybulakhite.

Constituent	Mean	Range	SD (2σ)	Reference material
NiO	26.21	24.87–27.09	0.96	Ni metal
CuO	11.99	9.69–13.74	1.53	Cu metal
MgO	1.86	0.96–2.42	0.22	MgO
CoO	0.72	0.46–1.00	0.55	Co metal
$C_2O_{3\,calc}$ [1]	40.15			
H_2O_{calc} [1]	20.09			
Total	101.03			

[1] Calculated by stoichiometry (2, 4 and 6 apfu for C, H and O, respectively).

Table 2. Powder X-ray diffraction pattern (d spacing in Å) of andreybulakhite and synthetic $Ni(C_2O_4) \cdot 2H_2O$. PDF denotes Powder Diffraction File. The three strongest PXRD lines are marked with bold.

Andreybulakhite		Synthetic $Ni(C_2O_4) \cdot 2H_2O$				Calculated XRD pattern				
		This study		PDF 00-025-0581						
I_{meas} [1]	d_{meas} [1]	I_{meas} [1]	d_{meas} [1]	I_{meas} [2]	d_{meas} [2]	I_{calc} [3]	d_{calc} [3]	h	k	l
100	**4.743**	100	4.723	100	4.720	100	4.7449	−2	0	0
						96	4.7226	−2	0	2
24	**3.946**	20	3.921	15	3.920	23	3.9420	0	0	2
8	3.572	> 1	3.559	13	3.570	31	3.5723	1	1	1
						8	3.5652	−1	1	2
29	**2.954**	22	2.949	45	2.942	54	2.9597	−4	0	2
3	2.709	1	2.668	1	2.710	1	2.7109	−3	1	3
6	2.646		2.668	13	2.637	7	2.6480	1	1	2
						26	2.6432	−1	1	3
12	2.530	10	2.5243	14	2.528	17	2.5252	0	2	1
7	2.2070	5	2.2035			12	2.2081	0	2	2
7	2.0665	7	2.0643	15	2.067	7	2.0670	−2	2	3
3	2.0460			9	2.035	12	2.0422	1	1	3
5	1.9118	5	1.9084	30	1.905	12	1.9163	−6	0	2
						11	1.9119	−6	0	4
6	1.8723	7	1.8644	13	1.866	15	1.8714	0	2	3
2	1.7809	1	1.7781	20	1.781	3	1.7826	−2	2	4
						7	1.7806	−5	1	5
3	1.7447					8	1.7467	1	3	0
1	1.6680			2	1.668	3	1.6671	−1	3	2
3	1.5834	3	1.5770	12	1.580	2	1.5847	0	2	4
				4	1.571	4	1.5793	−4	2	5
3	1.5397	1	1.5247	8	1.536	2	1.5392	−7	1	5
3	1.4803	2	1.4679	10	1.474	3	1.4799	−8	0	4
		1					1.3142	0	4	1
2	1.3140	1	1.3137			2	1.3140	0	0	6

[1] Rigaku R-Axis Rapid II diffractometer. [2] Experimental pattern of synthetic $Ni(C_2O_4) \cdot 2H_2O$ from Deyrieux et al. (1973) (PDF card no. 00-025-0581). [3] Theoretical XRD pattern calculated from structural data from Deyrieux et al. (1973).

growing on oxidized Cu–Ni ores. Associated minerals are plagioclase (anorthite), pyroxene (enstatite–ferrosilite series), chalcopyrite, pyrrhotite and pentlandite, the latter of which is most likely the source of nickel.

3 Optical properties and anthropotype synthesis

Optical properties were studied by means of a DLMP polarizing light microscope (Leica, Germany). Andreybulakhite forms platy to prismatic crystals up to $2 \times 1 \times 1$ µm in size that are combined into aggregates up to $40 \times 30 \times 30$ µm in

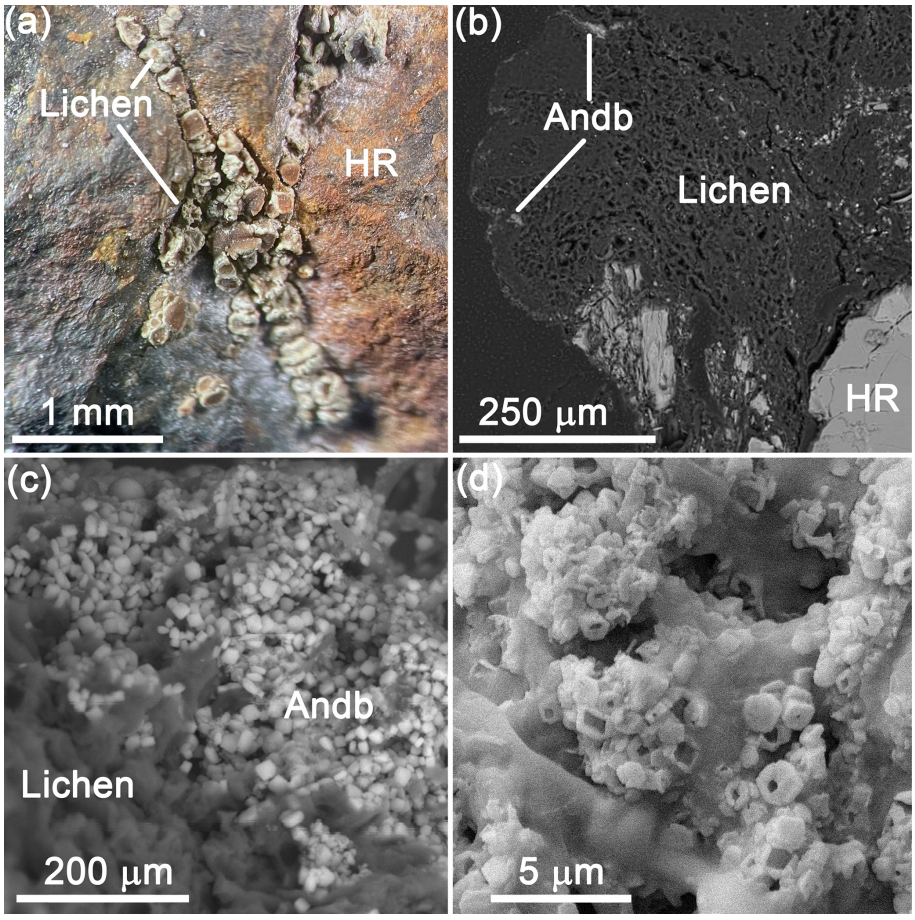

Figure 1. Andreybulakhite occurrence: **(a)** *Lecanora* cf. *polytropa* apothecia (lichen) on aggregate on sulfide ore (optical microscopy; host rock, HR); **(b)** andreybulakhite (Andb) aggregate inside lichen apothecia (scanning electron microscope (SEM) backscattered electron (BSE) image); **(c)** andreybulakhite crystals (SEM BSE image); **(d)** hopper-like andreybulakhite crystals (SEM secondary electron (SE) image).

size embedded in a lichen reproductive structure (apothecia) (Fig. 1). The mineral is colourless to pale green with vitreous lustre and non-fluorescent under either short- or long-wave ultraviolet radiation. The hardness of andreybulakhite could not be measured due to the small grain sizes but is likely ~ 1.5–2 by analogy with members of the humboldtine group (e.g. Giester et al., 2023). The calculated density is 2.420 g cm^{-3} based on the empirical formula (Table 1) and unit-cell parameters obtained from a powder X-ray diffraction (PXRD) study (Table 2). The mean refractive index calculated based on the Gladstone–Dale relationship is 1.594.

Due to the small amount of natural substance, as well as the very small size of the crystals $Ni(C_2O_4) \cdot 2H_2O$ powder was synthesized for direct comparison of X-ray and spectroscopic data. $Ni(C_2O_4) \cdot 2H_2O$ was synthesized in a water solution (500 mL volume) by adding $NiCl_2 \cdot 6H_2O$ (99.99 %, Sigma-Aldrich) into a solution of $Na_2C_2O_4$ (99.99 %, Sigma-Aldrich) at room temperature (23–25 °C) and a slightly acidic pH (6.0–7.2). The crystalline precipitate was filtered, washed with distilled water, dried at room temperature and checked for homogeneity by PXRD (Fig. 2).

4 Chemical composition

Elemental composition and morphology were studied by means of an S-3400N (Hitachi, Japan) scanning electron microscope (SEM) equipped with AZtec Energy X-Max 20 (Oxford Instruments, UK) energy-dispersive X-ray (EDX) and WAVE 500 (Oxford Instruments, UK) wavelength-dispersive X-ray (WDX) spectrometers. The conditions of the EDX analyses were 20 kV accelerating voltage, 2 nA beam current and 20 s data-collection time (excluding dead time). WDX analyses were acquired with 20 kV, 5 nA, 30 s per element and 30 s background acquisition times. Pure Co, Ni and Cu metals ($K\alpha$ lines); pyrite (Fe$K\alpha$ and S$K\alpha$); and MgO (Mg$K\alpha$) were used as analytical standards. The analyses of rock-forming minerals were completed using the same instrumental setup, with oxides and silicates as reference standards. It is important to note that

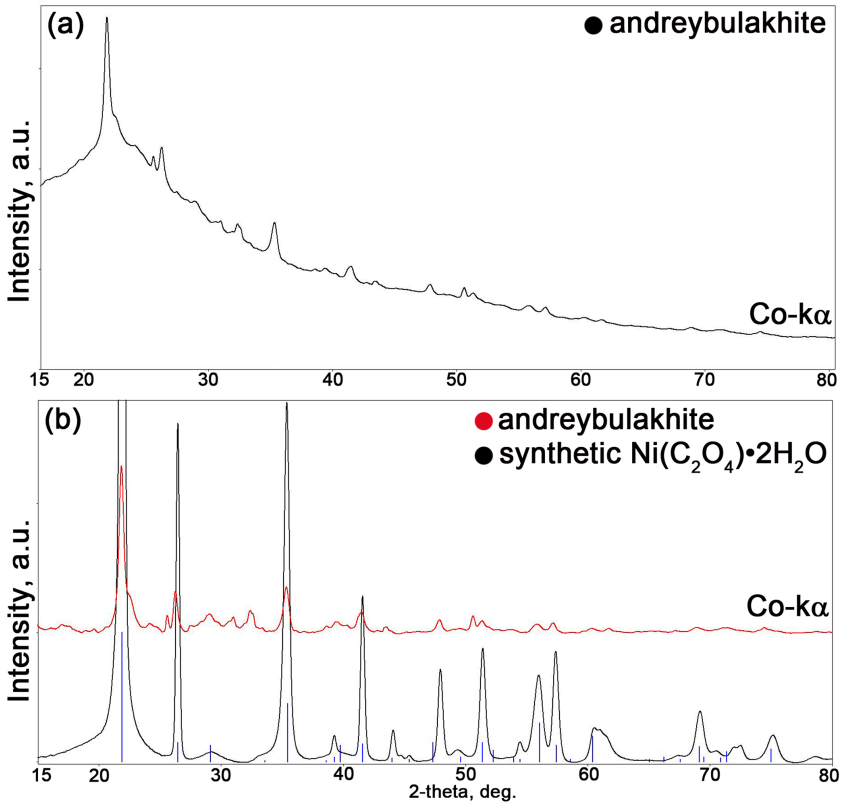

Figure 2. Fragment of the PXRD profile of andreybulakhite **(a, b)** and synthetic $Ni(C_2O_4) \cdot 2H_2O$ **(b)**: **(a)** raw profile and **(b)** background-subtracted profile. Note: blue lines are from PDF card no. 00-025-0581.

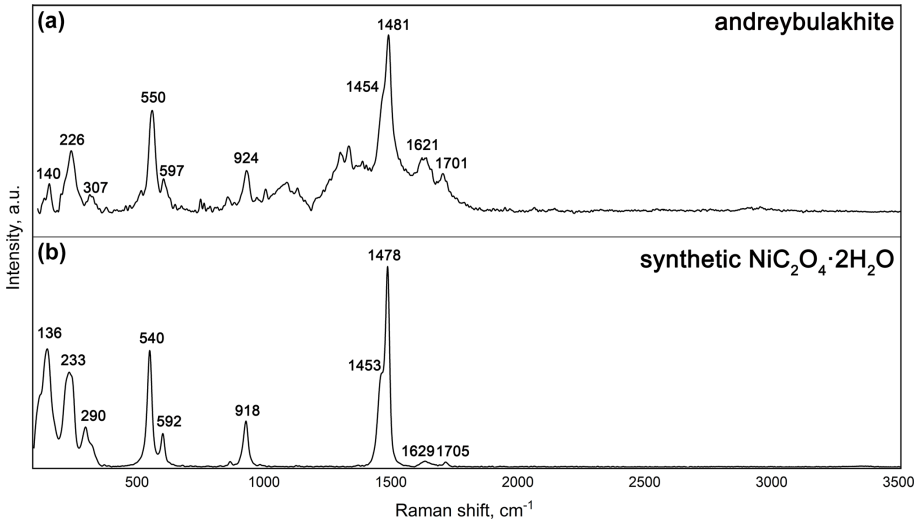

Figure 3. Raman spectra of andreybulakhite **(a)** and synthetic $Ni(C_2O_4) \cdot 2H_2O$ **(b)**.

the final chemical composition of andreybulakhite (Table 1) was measured (five spots) by EDX as a higher acquisition time ($\gg 30$ s) led to sample degradation. The water and C_2O_4 were confirmed by the presence of corresponding bands in the IR and Raman spectra of the mineral (Figs. 3, 4). The empirical formula calculated on the basis of $(Ni + Cu + Mg + Co) = 1$ atom per formula unit (apfu) is $(Ni_{0.63}Cu_{0.27}Mg_{0.08}Co_{0.02})_{\Sigma 1.00}\ (C_2O_4) \cdot 2H_2O$. The simplified formula is (Ni,Cu,Mg) $(C_2O_4) \cdot 2H_2O$, while the ideal formula is $Ni(C_2O_4) \cdot 2H_2O$, which requires NiO, 40.88 wt %; C_2O_3, 39.41 wt %; and H_2O, 19.71 wt % (total 100 wt %).

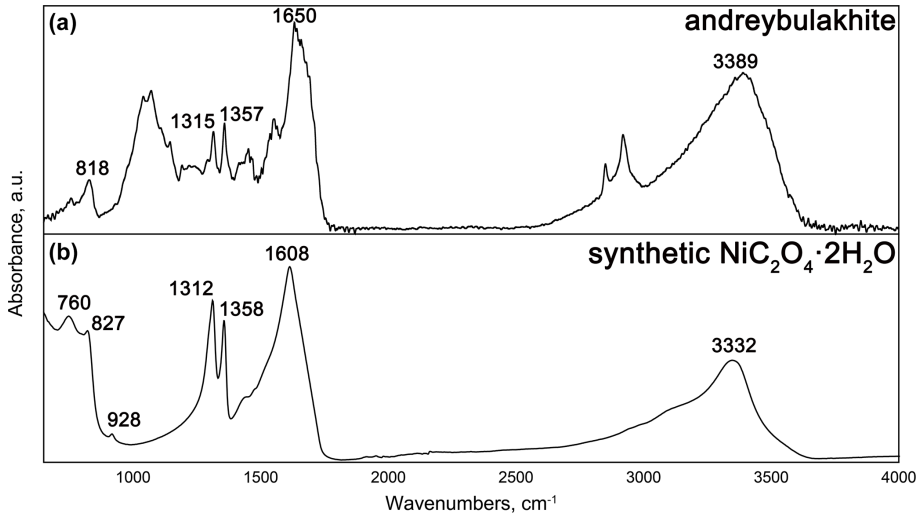

Figure 4. Infrared spectra of andreybulakhite **(a)** and synthetic $Ni(C_2O_4) \cdot 2H_2O$ **(b)**.

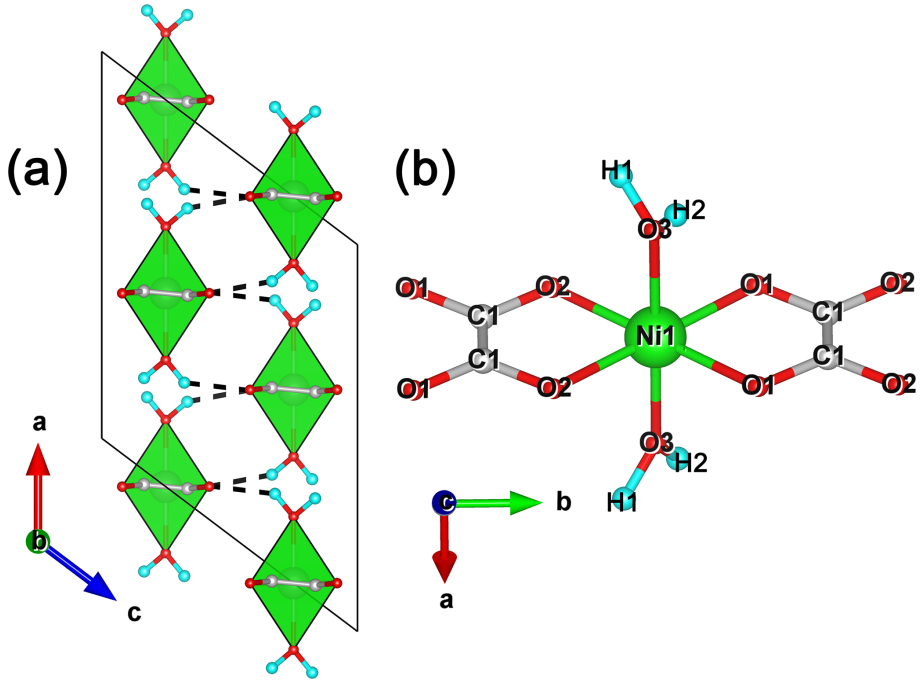

Figure 5. Crystal structure of synthetic $Ni(C_2O_4) \cdot 2H_2O$ (Puzan et al., 2018): **(a)** projected on (010) and **(b)** a fragment of the nickel oxalate chain. Note that NiO_6 polyhedra are visualized in green, H atoms are blue, O atoms are red and C atoms are grey. Hydrogen bonds are shown by dashed lines. The unit cell is outlined.

5 Powder X-ray diffraction data

Owing to the small size of available grains (1–2 µm), no single-crystal X-ray diffraction study was possible on andreybulakhite. PXRD data of andreybulakhite were obtained (Fig. 2) in Debye–Scherrer geometry by means of a Rigaku R-Axis Rapid II diffractometer equipped with a curved (cylindrical) imaging plate detector ($r = 127.4$ mm), using Co$K\alpha$ radiation ($\lambda = 1.79021$ Å) generated by a rotating anode (40 kV, 15 µA) with microfocus optics; exposure time was set to 60 min. Unit-cell parameters (monoclinic, space group $C2/c$) refined from powder data are $a = 11.8392(5)$ Å, $b = 5.3312(2)$ Å, $c = 9.8357(7)$ Å, $\beta = 126.723(5)°$, $V = 497.59(3)$ Å^3 and $Z = 4$.

Andreybulakhite belongs to a family of natural (humboldtine group) and synthetic oxalates with the general formula $M(C_2O_4) \cdot 2H_2O$ (M denotes Fe, Mn, Mg, Zn, Ni and Co). Their crystal structure (Fig. 5) contains chains of dis-

Table 3. Raman spectrum of andreybulakhite, synthetic $Ni(C_2O_4) \cdot 2H_2O$ and members of the humboldtine group.

$M(C_2O_4) \cdot 2H_2O$						Band assignment
M is Ni		M is Mg	M is Fe	M is Mn	M is Zn	
Andreybulakhite	Synthetic	Glushinskite	Humboldtite	Lindbergite	Katsarosite	
		3391 3367 3254	3315	3326	3353	OH stretching
1701	1730	1720 1660	1708			C=O stretching and/or multiphonon processes
1621	1632	1636 1612				H–OH bending vibrations
			1555			C–O and C–C
1454	1482 1457 1271 1065	1471 1454	1468 1450	1469	1473 1441	stretching
924	919	915 861	913 856	908	914	
	805					M–O stretching, C–C–O and O–C–O deformations
		657				
597	591	585	582	579	588	
550	540	527			537	
		521	518	517		
	353					M–O stretching
307	312 289	310 265	293 246			
	238	237		240		
226		226				
		221	203	198	204 132	
This study	Bickley et al. (1991)	Frost (2004)		Echigo and Kimata (2008)	Giester et al. (2023)	

torted octahedra $MO_4(H_2O)_2$ connected by flat oxalate ions (C_2O_4) acting as tetradentate ligands (Echigo and Kimata, 2010; Korneev et al., 2022; Puzan et al., 2018). According to previous studies (e.g. Deyrieux et al., 1973), two polymorphs are known: α-$Ni(C_2O_4) \cdot 2H_2O$ (space group (sp. gr.) $C2/c$) and β-$Ni(C_2O_4) \cdot 2H_2O$ (sp. gr. $Cccm$). β-$Ni(C_2O_4) \cdot 2H_2O$ is thermodynamically unstable and transforms into α-$Ni(C_2O_4) \cdot 2H_2O$ upon contact with a solution containing an excess of oxalate ions (Deyrieux et al., 1973).

6 Spectroscopy

6.1 Raman spectroscopy

The Raman spectra of andreybulakhite and synthetic $Ni(C_2O_4) \cdot 2H_2O$ (Fig. 3) were obtained by means of a SENTERRA (Bruker, Germany) confocal Raman spectrometer conjugated with a BX51 microscope (Olympus, Japan) in backscattering geometry. The Raman spectrometer is equipped with a solid-state laser ($\lambda = 785$ nm). In order to perform simultaneously safe Raman measurements of biological media and oxalate mineral, the laser power was reduced to 0.3 mW under the 20× objective with numerical aperture 0.4. The spectrum was obtained in a range of 80–3700 cm^{-1} at a resolution of about 3 cm^{-1} and room temperature. To improve the signal-to-noise ratio, the time of acquisition was 150 s with eight repetitions.

The Raman spectrum of andreybulakhite (Fig. 3) contains the following bands (cm^{-1}): 1701 (C=O stretching vibrations and/or multiphonon processes); 1621 (H_2O bending vibrations); 1454 and 924 (C–O stretching, C–C stretching);

Table 4. IR spectrum of andreybulakhite, synthetic $Ni(C_2O_4) \cdot 2H_2O$ and members of the humboldtine group.

$M(C_2O_4) \cdot 2H_2O$					Band assignment
M is Ni		*M* is Mg	*M* is Fe	*M* is Mn	
Andreybulakhite	Synthetic	Glushinskite	Humboldtite	Lindbergite	
			3472		OH stretching
3389	3360	3389	3312		
		3380			
		3360			
		3305			
		3230			
	3160	3126	3136	3155	
				3089	H–OH bending vibrations
				2978	
				2944	
				2820	
				2773	
		1679			
1650	1660	1660	1656	1655	
		1634			
	1610	1603	1615	1604	C–O and C–C stretching
	1560	1580	1514		
	1475		1479		
	1445				
1357	1357	1369	1357	1359	
1315	1316	1322	1312	1310	
		1314	1301		
	915	1169	1266		
	840				
818	825	827	818		*M*–O stretching, C–C–O and O–C–O deformations
		803	766		
		684	715		
	545				*M*–O stretching
	492				
	368				
	330				
	290				
	260				
	204				
This study	Bickley et al. (1991)	Frost (2004)		Echigo and Kimata (2008)	

597 (Ni–O stretching, C–C–O and O–C–O bending vibrations); 550, 307 and 226 (Ni–O stretching and bending vibrations). The band assignments were made by analogy with the Raman spectra of synthetic $Ni(C_2O_4) \cdot 2H_2O$ (Bickley et al., 1991) and other members of the humboldtine group (Frost, 2004; Echigo and Kimata, 2008). The andreybulakhite spectrum is similar to the spectrum of synthetic $Ni(C_2O_4) \cdot 2H_2O$ obtained by us and close to that obtained by Bickley et al. (1991) (Table 3). The observed differences (Raman band

Table 5. Selected crystallographic data for andreybulakhite, synthetic $Ni(C_2O_4) \cdot 2H_2O$ and members of the humboldtine group.

	$M(C_2O_4) \cdot 2H_2O$					
	M = Ni		M is Fe	M is Mg	M is Mn	M is Zn
	Andreybulakhite	Synthetic	Humboldtite	Glushinskite	Lindbergite	Katsarosite
Sp. gr.			$C2/c$			
a (Å)	11.8393	11.7748	12.060	12.675	11.995	11.768
b (Å)	5.3312	5.3328	5.550	5.406	5.632	5.388
c (Å)	9.8357	9.8326	9.804	9.984	9.967	9.804
β (°)	126.72	127.21	127.97	129.45	128.34	127.045
Z			4			
Reference	This study	Deyrieux et al. (1973)	Caric (1959)	Wilson et al. (1980)	Atencio et al. (2004)	Giester et al. (2023)

shift; Table 3) are most likely associated with Cu for Ni substitution.

6.2 Infrared spectroscopy

Fourier-transform (FT) infrared (IR) spectra of andreybulakhite and synthetic $Ni(C_2O_4) \cdot 2H_2O$ (Fig. 4) were obtained using a HYPERION 2000 confocal IR microscope (Bruker, Germany) attached to a VERTEX 70 spectrometer (Bruker, USA). Aggregate of andreybulakhite crystals with host lichen and powder of $Ni(C_2O_4) \cdot 2H_2O$ crystals was placed onto a polished KBr disc, and the spectra were recorded in transmission mode, with a 15× reflector objective and 30 µm square aperture. The wavenumber range was between 4000 and 650 cm^{-1}, with a spectral resolution of 4 cm^{-1} and averaging over 42 scans.

The IR spectrum of andreybulakhite contains the following bands (cm^{-1}): 3389 (O–H stretching vibrations of OH groups), 1640 (H_2O bending vibrations), 1357 and 1315 (C–O and C–C stretching), and 818 (Ni–O, C–O and C–C stretching, C–C–O and O–C–O bending vibrations). The band assignments were made by analogy with the IR spectra of synthetic $Ni(C_2O_4) \cdot 2H_2O$ (Bickley et al., 1991) and other members of the humboldtine group (Echigo and Kimata, 2008; Frost, 2004). The andreybulakhite IR spectrum is similar to the IR spectrum of synthetic $Ni(C_2O_4) \cdot 2H_2O$ obtained by us and close to that obtained by Bickley et al. (1991) (Table 4). The observed differences (IR band shift; Table 4) are most likely associated with Cu for Ni substitution in the sample, as well as a significant contribution of the organic components of the lichen.

7 Discussion and conclusions

Andreybulakhite ($Ni^{2+}(C_2O_4) \cdot 2H_2O$) belongs to the humboldtine group, which includes humboldtine, $Fe^{2+}(C_2O_4) \cdot 2H_2O$; lindbergite, $Mn^{2+}(C_2O_4) \cdot 2H_2O$; glushinskite, $Mg(C_2O_4) \cdot 2H_2O$; and recently discovered katsarosite, $Zn^{2+}(C_2O_4) \cdot 2H_2O$. Andreybulakhite has biogenic origin, which is also the case for lindbergite (e.g. Wilson and Jones, 1984) and glushinskite (e.g. Wilson et al., 1980). It is interesting to note that almost all works on natural oxalates point to their biologically induced origin, although often the organism source of oxalic acid cannot be identified (e.g. Giester et al., 2023). This is partly due to the specificity of mineralogical and lichenological studies. Mineralogists traditionally do not work with purely biological matter (for example, fruiting bodies of lichens), while lichenologists do not describe new minerals. The most promising approach in the search for such minerals is the collective work of geologists and botanists, which allows the identification of interesting phases and the competent characterization of them.

It is also interesting to note that despite the fact that oxalate finds are traditionally associated with the activity of living organisms (both flora and fauna; e.g. Gadd et al., 2014; Giester et al., 2023; Vereshchagin et al., 2023), some oxalates are clearly abiogenic in nature. Thus, natroxalate, $Na_2(C_2O_4)$, and kyanoxalite, $Na_7(Al_{6-x}Si_{6+x}O_{24})(C_2O_4)_{0.5+x} \cdot 5H_2O$ ($0 < x < 0.5$), were found in ultra-alkaline pegmatites formed under conditions of high temperatures and fairly high pressures (e.g. Khomyakov, 1996; Chukanov et al., 2010). Nevertheless, on modern Earth, such conditions are realized much less frequently than biological weathering of rocks, which is widespread on all continents and across all types of rocks.

An interesting feature of andreybulakhite is its chemical composition. Andreybulakhite does not contain iron (Table 1). The absence of iron in the mineral is the result of natural nickel refining in near-surface conditions due to oxidation processes of primary Fe-, Ni- and Cu-rich ore. The primary source of nickel (and copper) is iron sulfides (see above). Their oxidation by acids leads to the formation of solutions in which iron is easily oxidized to the trivalent state and then does not enter into humboldtine-type oxalates (e.g. Deyrieux et al., 1973; Dubernat and Pezerat, 1974; Echigo

and Kimata, 2010). The same process resulted in the appearance of morenosite, $Ni(SO_4) \cdot 7H_2O$, which was found on the surface of oxidized Cu–Ni ores of the Nyud-II deposit (Igor V. Pekov, personal communication, 2020). There are Mg-rich (epsomite) and Zn-rich (goslarite) members of the epsomite group, but no Fe-rich member has so far been identified. Nickelhexahydrite, $Ni(SO_4) \cdot 6H_2O$, is another Ni-rich sulfate found on the surface of oxidized Cu–Ni ores of the Nyud-II deposit. Its formation is most likely associated with the dehydration of morenosite, which is indicated by the high Ni : Fe ratio (up to 10 : 1).

Another interesting feature of the chemical composition of andreybulakhite is the high Cu content and the presence of Mg and Co in its composition (Table 1). There are no data on the possibility of the existence of a copper analogue of humboldtine. The only data available are on $Ni_{x/3}Cu_{y/3}Mn_{(3-x-y)/3}(C_2O_4)n \cdot H_2O$ oxalates (Drouet et al., 1999), which indirectly indicates the possibility of the existence of limited solid $Ni_{1-x}Cu_x(C_2O_4) \cdot 2H_2O$ solutions. Our preliminary results on synthesis in the NiO–CuO–C_2O_3–H_2O system confirm this assumption and indicate the presence of an isodimorphic andreybulakhite–moolooite transition. It is worth noting that the study of Chen et al. (2019) showed the presence of a complete solid solution in the $Co_{1-x}Ni_xC_2O_4 \cdot 2H_2O$ series. Both $Ni(C_2O_4) \cdot 2H_2O$ and $Co(C_2O_4) \cdot 2H_2O$ were synthesized with the participation of *Aspergillus niger* (Magyarosy et al., 2002; Ferrier et al., 2021), which confirms the possibility of nickel and cobalt oxalate formation in biofilms and indicates a high probability of detecting the cobalt analogue of humboldtine in nature. The presence of solid solution in the $Mg_{1-x}Ni_xC_2O_4 \cdot 2H_2O$ series is confirmed in natural samples (e.g. Wilson et al., 1980).

Data availability. All the data are provided in the article. Raw data (e.g. Raman spectra) can be obtained on request.

Author contributions. OSV observed the unknown mineral. OSV, SNB and DVP collected and interpreted spectroscopic data. SNB and MGK carried out the X-ray diffraction experiments and executed structural refinements. OSV and NSV performed the microprobe analyses. MSZ identified the type of lichen and selected areas most enriched with oxalates. MAK performed anthropotype synthesis. OSV, SNB and OVFK wrote the text, in consultation with all authors.

Competing interests. The contact author has declared that none of the authors has any competing interests.

Disclaimer. Publisher's note: Copernicus Publications remains neutral with regard to jurisdictional claims made in the text, published maps, institutional affiliations, or any other geographical representation in this paper. While Copernicus Publications makes every effort to include appropriate place names, the final responsibility lies with the authors.

Special issue statement. This article is part of the special issue "New minerals: EJM support". It is not associated with a conference.

Acknowledgements. The work was carried out using the analytical capabilities of the resource centres of St Petersburg State University: the Centre for X-Ray Diffraction Studies, the Centre for Optical and Laser Materials Research, the Centre for Geo-Environmental Research and Modelling (GEOMODEL), and the Centre for Microscopy and Microanalysis. XRD studies were done at the Centre for X-Ray Diffraction Studies within the project AAAA-A19-119091190094-6. The authors are grateful to Gabriela Ferracutti and Ole William Purvis for their careful examination of the manuscript contents and positive feedback. The authors express their gratitude to the handling chief editor Sergey V. Krivovichev for editorial handing of this contribution.

Financial support. Publisher's note: the article processing charges for this publication were not paid by a Russian or Belarusian institution.

Review statement. This paper was edited by Sergey Krivovichev and reviewed by Ole William Purvis and Gabriela Ferracutti.

References

Adamo, P. and Violante, P.: Weathering of rocks and neogenesis of minerals associated with lichen activity, Appl. Clay Sci., 16, 229–256, https://doi.org/10.1016/S0169-1317(99)00056-3, 2000.

Atencio, D., Coutinho, J. M. V., Graeser, S., Matioli, P. A., and Filho, L. A. D. M.: Lindbergite, a new Mn oxalate dihydrate from Boca Rica mine, Galiléia, Minas Gerais, Brazil, and other occurrences, Am. Mineral., 89, 1087–1091, https://doi.org/10.2138/am-2004-0721, 2004.

Bickley, R. I., Edwards, H. G. M., and Rose, S. J.: A Raman spectroscopic study of nickel(II) oxalate dihydrate, $NiC_2O_4 \cdot 2H_2O$ and dipotassium bisoxalatonickel(II) hexahydrate, $K_2Ni(C_2O_4)_2 \cdot 6H_2O$, J. Mol. Struct., 243, 341–350, https://doi.org/10.1016/0022-2860(91)87048-M, 1991.

Breithaupt, A.: Kurze Charakteristik des Mineral-System's, 8, Freiberg, 75 pp., 1820.

Bulakh, A., Harma, P., Panova, E., and Selonen, O.: Rapakivi granite in the architecture of St Petersburg: A potential global heritage stone from Finland and Russia, in: Geological Society Special Publication, vol. 486, Geological Society of London, 67–76, https://doi.org/10.1144/SP486-2018-5, 2020.

Bulakh, A. G. and Ivanikov, V. V: Carbonatites of the Turi Peninsula, Kola; role of magmatism and of metasomatism, Can. Mineral., 34, 403–409, 1996.

Bulakh, A. G., Nesterov, A. R., Williams, C. T., and Anisimov, I. S.: Zirkelite from the Sebl'yavr carbonatite complex, Kola Peninsula, Russia: an X-ray and electron microprobe study of a partially metamict mineral, Mineral. Mag., 62, 837–846, https://doi.org/10.1180/002646198548205, 1998.

Burford, E. P., Fomina, M., and Gadd, G. M.: Fungal involvement in bioweathering and biotransformation of rocks and minerals, Mineral. Mag., 67, 1127–1155, https://doi.org/10.1180/0026461036760154, 2003.

Caric, S.: Amélioration de la structure de la humboldtine FeC_2O_4. 2 H_2O, B. Soc. Fr. Mineral. Cr., 82, 50–55, https://doi.org/10.3406/bulmi.1959.5304, 1959.

Chashchin, V. V. and Ivanchenko, V. N.: Sulfide PGE–Cu–Ni and Low-Sulfide Pt–Pd Ores of the Monchegorsk Ore District (Arctic Western Sector): Geology, Mineralogy, Geochemistry, and Genesis, Russ. Geol. Geophys., 63, 519–542, https://doi.org/10.2113/RGG20214410, 2022.

Chashchin, V. V., Savchenko, Y. E., Petrov, S. V., and Kiseleva, D. V.: Platinum content and formation conditions of the sulfide PGE–Cu–Ni Nyud-II deposit of the Monchegorsk pluton, Kola peninsula, Russia, Geol. Ore Deposit., 2, 87–117, 2021.

Chashchin, V. V., Karinen, T., and Savchenko, Y. E.: Location, chemical content, and origin of Loveringite from Paleoproterozoic layered intrusions of the Fennoscandian Shield: The Syöte block of the Koillismaa, Finland, and the Nyud of the Monchegorsk pluton, Russia, Lithos, 442–443, 107073, https://doi.org/10.1016/j.lithos.2023.107073, 2023.

Chen, T. H., Liu, Z. S., Fan, H. L., Guo, L. T., and Tao, X.: Optimization design of orthorhombic-monoclinic Co_1-xNixC_2O_4· $2H_2O$ solid solutions for high-performance pseudocapacitors, J. Alloy. Compd., 808, 151722, https://doi.org/10.1016/j.jallcom.2019.151722, 2019.

Chukanov, N. V., Pekov, I. V., Olysych, L. V., Massa, W., Yakubovich, O. V., Zadov, A. E., Rastsvetaeva, R. K., and Vigasina, M. F.: Kyanoxalite, a new cancrinite-group mineral species with extraframework oxalate anion from the Lovozero alkaline pluton, Kola Peninsula, Geol. Ore Deposit., 52, 778–790, https://doi.org/10.1134/S107570151008009X, 2010.

Clarke, R. M. and Williams, I. R.: Moolooite, a naturally occurring hydrated copper oxalate from Western Australia, Mineral. Mag., 50, 295–298, https://doi.org/10.1180/minmag.1986.050.356.15, 1986.

Deyrieux, R., Berro, C., and Peneloux, A.: Studies on oxalates of some bivalent metals .3. Crystal-structure of dihydrated manganese, cobalt, nickel and zinc oxalates - -polymorphism of dihydrated cobalt and nickel oxalates, Bull. la Société Chim. Paris, 6, 25–34, 1973.

Drouet, C., Alphonse, P., and Rousset, A.: Synthesis and characterization of non-stoichiometric nickel-copper manganites, Solid State Ionics, 123, 25–37, https://doi.org/10.1016/S0167-2738(99)00106-X, 1999.

Dubernat, J. and Pezerat, H.: Fautes d'Empilement dans les Oxalates Dihydratés des métaux divalents de la série magnésienne (Mg,Fe,Co,Ni,Zn,Mn), J. Appl. Crystallogr., 7, 387–393, https://doi.org/10.1107/S0021889874009861, 1974.

Echigo, T. and Kimata, M.: Single-crystal X-ray diffraction and spectroscopic studies on humboldtine and lindbergite: weak Jahn-Teller effect of Fe^{2+} ion, Phys. Chem. Miner., 35, 467–475, https://doi.org/10.1007/s00269-008-0241-7, 2008.

Echigo, T. and Kimata, M.: Crystal chemistry and genesis of organic minerals: A review of oxalate and polycyclic aromatic hydrocarbon minerals, Can. Mineral., 48, 1329–1358, https://doi.org/10.3749/canmin.48.5.1329, December 2010.

Estroff, L. A.: Introduction: Biomineralization, Chem. Rev., 108, 4329–4331, https://doi.org/10.1021/cr8004789, 2008.

Ferrier, J., Csetenyi, L., and Gadd, G. M.: Selective fungal bioprecipitation of cobalt and nickel for multiple-product metal recovery, Microb. Biotechnol., 14, 1747–1756, https://doi.org/10.1111/1751-7915.13843, 2021.

Fersman, A. E.: Mineral resources of the Kola Peninsula: Current status, analysis, forecast, Publisher of the USSR Academy of Sciences, Moscow-Leningrad, 345 pp., 1941.

Fomina, M., Hillier, S., Charnock, J. M., Melville, K., Alexander, I. J., and Gadd, G. M.: Role of oxalic acid overexcretion in transformations of toxic metal minerals by Beauveria caledonica, Appl. Environ. Microb., 71, 371–381, https://doi.org/10.1128/AEM.71.1.371-381.2005, 2005.

Frank-Kamenetskaya, O. V, Ivanyuk, G. Y., Zelenskaya, M. S., Izatulina, A. R., Kalashnikov, A. O., Vlasov, D. Y., and Polyanskaya, E. I.: Calcium oxalates in lichens on surface of apatite-nepheline ore (Kola Peninsula, Russia), Minerals, 9, 1–13, https://doi.org/10.3390/min9110656, 2019.

Frank-Kamenetskaya, O. V., Zelenskaya, M. S., Izatulina, A. R., Vereshchagin, O. S., Vlasov, D. Y., Himelbrant, D. E., and Pankin, D. V.: Copper oxalate formation by lichens and fungi, Sci. Rep., 11, 24239, https://doi.org/10.1038/s41598-021-03600-5, 2021.

Frost, R. L.: Raman spectroscopy of natural oxalates, Anal. Chim. Ac., 517, 207–214, https://doi.org/10.1016/j.aca.2004.04.036, 2004.

Gadd, G. M., Bahri-Esfahani, J., Li, Q., Rhee, Y. J., Wei, Z., Fomina, M., and Liang, X.: Oxalate production by fungi: significance in geomycology, biodeterioration and bioremediation, Fungal Biol. Rev., 28, 36–55, https://doi.org/10.1016/j.fbr.2014.05.001, 2014.

Genkin, A. D., Zhuravlev, N. N., and Smirnova, E. M.: Moncheite and kotulskite – new minerals – and the composition of michenerite, Zap. Vsesoyuznogo Mineral. Obs., 92, 33–50, 1963.

Giester, G., Rieck, B., Lengauer, C. L., Kolitsch, U., and Nasdala, L.: Katsarosite $Zn(C_2O_4)$· $2H_2O$, a new humboldtine-group mineral from the Lavrion Mining District, Greece, Mineral. Petrol., 117, 259–267, https://doi.org/10.1007/s00710-023-00810-9, 2023.

Gorbunov, G. E., Bel'kov, E. V., Makievsky, S. E., and Goryainov, P. M.: Mineral deposits of the Kola Peninsula, Nauka, Leningrad, 272 pp., 1981.

Grokhovskaya, T. L., Karimova, O. V., Vymazalová, A., Laufek, F., Chareev, D. A., Kovalchuk, E. V., Magazina, L. O., and Rassulov, V. A.: Nipalarsite, $Ni_8Pd_3As_4$, a new platinum-group mineral from the Monchetundra Intrusion, Kola Peninsula, Russia, Mineral. Mag., 83, 837–845, https://doi.org/10.1180/mgm.2019.70, 2019.

Huang, Y., Zhang, L., Yuan, S., Liu, W., Zhang, C., Tian, D., and Ye, X.: The Production of Oxalate by *Aspergillus niger* under Different Lead Concentrations, Agronomy, 13, 1182, https://doi.org/10.3390/agronomy13041182, 2023.

Jarosz-Wilkolazka, A. and Gadd, G. M.: Oxalate production by wood-rotting fungi growing in toxic metal-amended medium,

Chemosphere, 52, 541–547, https://doi.org/10.1016/S0045-6535(03)00235-2, 2003.

Karykowski, T., Maier, W. D., Mcdonald, I., Groshev, N. Y., Pripachkin, P. V., Barnes, S. J., and Savard, D.: Critical controls on the formation of contact-style PGE-Ni-Cu mineralization: Evidence from the Paleoproterozoic Monchegorsk Complex, Kola Region, Russia, Econ. Geol. Bull. Soc., 113, 911–935, https://doi.org/10.5382/econgeo.2018.4576, 2018.

Khomyakov, A. P.: Natroxalate $Na_2C_2O_4$ – a new mineral, Zap. Vseross. Mineral. Obs., 125, 126–132, 1996.

Korneev, A. V., Izatulina, A. R., Kuz'mina, M. A., and Frank-Kamenetskaya, O. V.: Solid Solutions of Lindbergite–Glushinskite Series: Synthesis, Ionic Substitutions, Phase Transformation and Crystal Morphology, Int. J. Mol. Sci., 23, 14734, https://doi.org/10.3390/ijms232314734, 2022.

Krivovichev, V. G.: Mineral species, St. Petersburg State University press, 600 pp., ISBN 978-5-288-06121-9, 2021 (in Russian).

Magyarosy, A., Laidlaw, R., Kilaas, R., Echer, C., Clark, D., and Keasling, J.: Nickel accumulation and nickel oxalate precipitation by *Aspergillus niger*, Appl. Microbiol. Biot., 59, 382–388, https://doi.org/10.1007/s00253-002-1020-x, 2002.

Purvis, O. W.: The Occurrence of Copper Oxalate in Lichens Growing on Copper Sulphide-Bearing Rocks In Scandinavia, Lichenologist, 16, 197–204, https://doi.org/10.1017/S0024282984000347, 1984.

Purvis, O. W.: Adaptation and interaction of saxicolous crustose lichens with metals, Bot. Stud., 55, 23, https://doi.org/10.1186/1999-3110-55-23, 2014.

Puzan, A. N., Baumer, V. N., Lisovytskiy, D. V., and Mateychenko, P. V.: Structure transformations in nickel oxalate dihydrate $NiC_2O_4 \cdot 2H_2O$ and nickel formate dihydrate $Ni(HCO_2)_2 \cdot 2H_2O$ during thermal decomposition, J. Solid State Chem., 266, 133–142, https://doi.org/10.1016/j.jssc.2018.07.005, 2018.

Ralph, J., Von Bargen, D., Martynov, P., Zhang, J., Que, X., Prabhu, A., Morrison, S.M., Li, W., Chen, W., and Ma, X.: Mindat.org – the open access mineralogy database to accelerate data-intensive geoscience research, Am. Mineral., https://doi.org/10.2138/am-2024-9486, 2024.

van Zuijlen, K., Roos, R. E., Klanderud, K., Lang, S. I., and Asplund, J.: Mat-forming lichens affect microclimate and litter decomposition by different mechanisms, Fungal Ecol., 44, 100905, https://doi.org/10.1016/j.funeco.2019.100905, 2020.

Vereshchagin, O. S., Frank-kamenetskaya, O. V, Yu, D., Zelenskaya, M. S., Rodina, O. A., Chernyshova, I. A., Himelbrant, D. E., Stepanchikova, I. S., and Britvin, S. N.: Microbial biomineralization under extreme conditions: case study of basaltic rocks, Tolbachik Volcano, Kamchatka, Russia, Catena, 226, 107048, https://doi.org/10.1016/j.catena.2023.107048, 2023.

Vlasov, D. Y., Frank-Kamenetskaya, O. V., Zelenskaya, M. S., Sazanova (nee Barinova), K. V., Rusakov, A. V., and Izatulina, A. R.: The use of *Aspergillus niger* in modeling of modern mineral formation in lithobiotic systems, in: *Aspergillus niger*, Pathogenicity, cultivation and uses, edited by: Baughan, E., Nova Publisher, New York, 1–123, ISBN 978-1-53618-080-0, 2020.

Vymazalová, A., Laufek, F., Grokhovskaya, T. L., and Stanley, C. J.: Monchetundraite, Pd_2NiTe_2, a new mineral from the Monchetundra layered intrusion, Kola Peninsula, Russia, Mineral. Petrol., 114, 263–271, https://doi.org/10.1007/s00710-020-00698-9, 2020.

Wenk, H.-R. and Bulakh, A. G.: Minerals. Their constitution and origin, Cambridge University Press, 621 pp., ISBN 978-0-521-82238-1, 2016.

Wilson, M. J. and Jones, D.: The occurrence and significance of manganese oxalate in Pertusaria coralline (Lichenes), Pedobiologia, 26, 373–279, 1984.

Wilson, M. J., Jones, D., and Russell, J. D.: Glushinskite, a naturally occurring magnesium oxalate, Mineral. Mag., 43, 837–840, https://doi.org/10.1180/minmag.1980.043.331.02, 1980.